

Supporting information:

Organic Metal – Organic Semiconductor Blended Contacts in Single Crystal Field-Effect Transistors for a Significant Improvement of the Device Performance

Device fabrication and OFET characterisation:

Performing four probe DC measurements on the TTF-TCNQ electrodes a conductivity of $\sigma=1.6\text{ S/cm}$ was found. The X-ray diffraction pattern of freshly evaporated TTF-TCNQ electrodes deposited on Si/SiO₂ is shown in **Figure S1**.

Figure S2 shows the device characteristics of a typical TC DT-TTF single crystal OFET, where the source drain current was swept forwards and backwards. Hardly any hysteresis was observed. **Figure S3** depicts one of the best performing device based on the BC architecture where the DT-TTF single crystal was grown from a toluene solution on top of the TTF-TCNQ electrodes. Note that due to the smaller channel dimensions in this case the source drain voltage, as well as the source gate voltage was swept only up to -15 V.

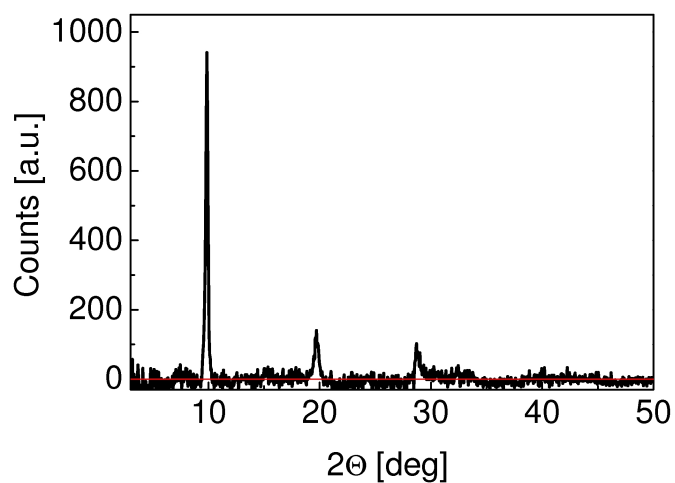


Figure S1: X-Ray diffractogram of freshly evaporated TTF-TCNQ electrodes deposited on a Si/SiO₂ substrate.

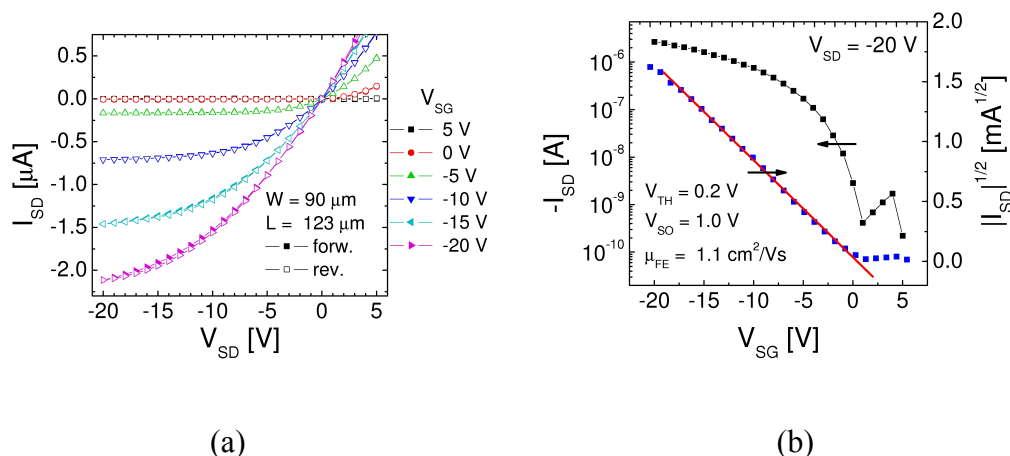


Figure S2: TC DT-TTF single crystal OFET with top evaporated TTF-TCNQ source and drain electrodes. For this device, the channel dimensions were found to be $W=90\mu\text{m}$ and $L=123 \mu\text{m}$, for width and length, respectively. a) Output and b) transfer characteristics.

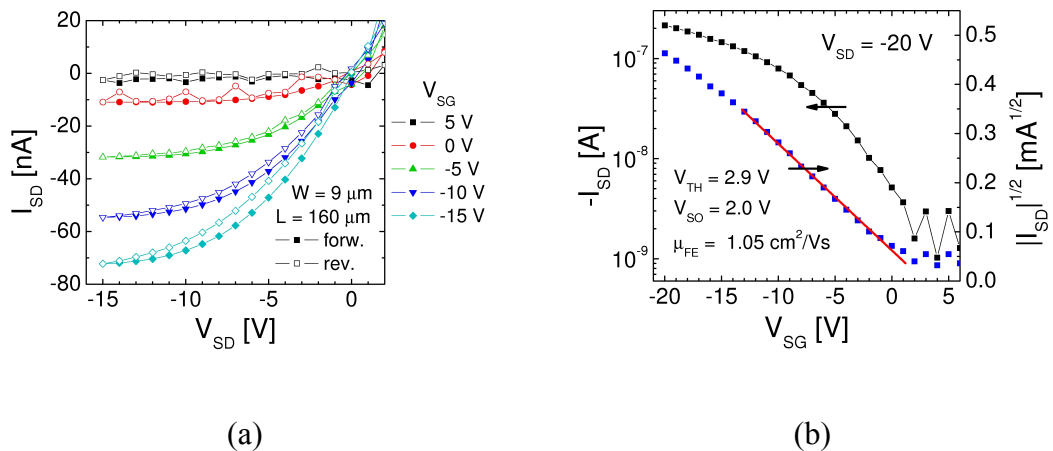


Figure S3: BC DT-TTF single crystal OFET based on DT-TTF grown from toluene on top of organic TTF-TCNQ source and drain electrodes. For this device, the channel dimensions were found to be $W = 9 \mu\text{m}$ and $L = 160 \mu\text{m}$, for width and length, respectively. a) Output and b) transfer characteristics.

Raman studies of the interface at the junction of the single crystal and the organic electrode:

In **Figure S4** the confocal Raman spectra of a PhCl grown BC DT-TTF OFET with TTF-TCNQ electrodes are reported between 300 and 1700 cm⁻¹. In this range we can detect the characteristic bands of the intramolecular modes of both the organic and the electrode. We indeed see an extended spectral overlap in their contact area. As explained in the caption of the Figure, the spectral analysis has allowed us to disentangle the spectral profiles and to verify that in the overlapping region they can always been resolved as the sum of the spectra of the pure compounds DT-TTF and TTF-TCNQ. This is evident from the difference spectrum c) of the Figure, which matches the DT-TTF crystal spectrum.

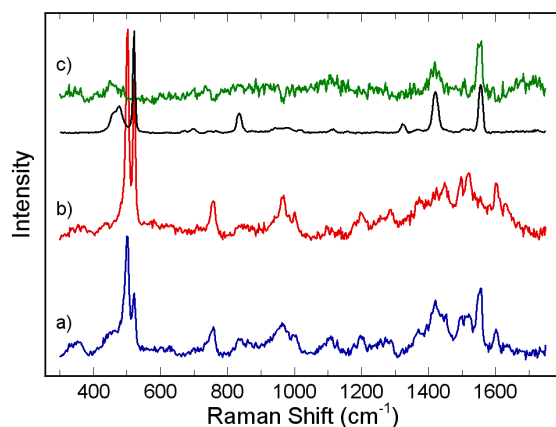


Figure S4. Confocal Raman spectra of a PhCl grown BC DT-TTF OFET with TTF-TCNQ electrodes. From bottom to top: a) spectrum of a DT-TTF single crystal collected in an area of TTF-TCNQ/DT-TTF contact and therefore showing both the bands of DT-TTF and the TTF-TCNQ electrode; b) spectrum of the TTF-TCNQ electrode; c) difference spectrum a)–b), compared with the spectrum of a DT-TTF single crystal obtained far from the TTF-TCNQ electrode area (black trace).

A detailed analysis of the region 1350–1650 cm⁻¹ is reported in **Figure S5**. This range is relevant to our analysis because it is especially sensitive to the occurrence of a chemical reaction of DT-TTF (i.e. oxidation). The outcome of the deconvolution of the spectral profiles allows us to rule out any possible chemical modification in the contact area.

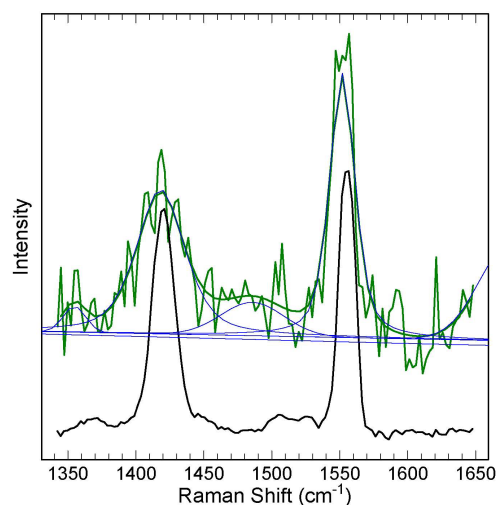


Figure S5. Upper trace: confocal Raman spectra of a PhCl grown BC DT-TTF OFET with TTF-TCNQ electrodes in the enlarged region $1350\text{--}1650\text{ cm}^{-1}$ of the difference spectrum c) of the previous Figure. The fit of the spectrum and its deconvolution are also reported. Bottom trace: reference spectrum of a pure DT-TTF single crystal.

AFM - Analysis of single crystal OFETs based on DT-TTF as active material:

To obtain more information from the morphological point of view, Atomic Force Microscopy (AFM) of the single crystal OFETs and the related interfaces were preformed on a 5500LS SPM system from Agilent Technologies. **Figure S6** shows an AFM image of a toluene grown DT-TTF single crystal OFET, where the crystal clearly continues on top of the organic electrode.

Figure S7 shows the AFM image of the best performing OFET measured in the channel region of the device, where the DT-TTF single crystal can be easily identified.

Figure S8 shows the corresponding AFM image of a PhCl grown DT-TTF single crystal, where the crystal melts into the organic electrode.

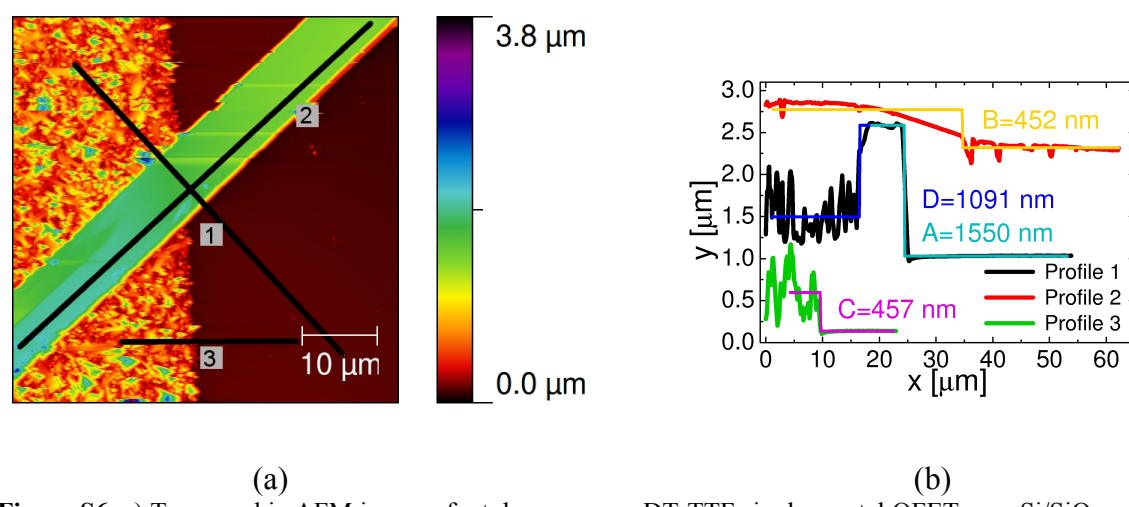


Figure S6. a) Topographic AFM image of a toluene grown DT-TTF single crystal OFET on a Si/SiO₂ and TTF-TCNQ electrodes. The single crystal continues on top of the organic electrode.

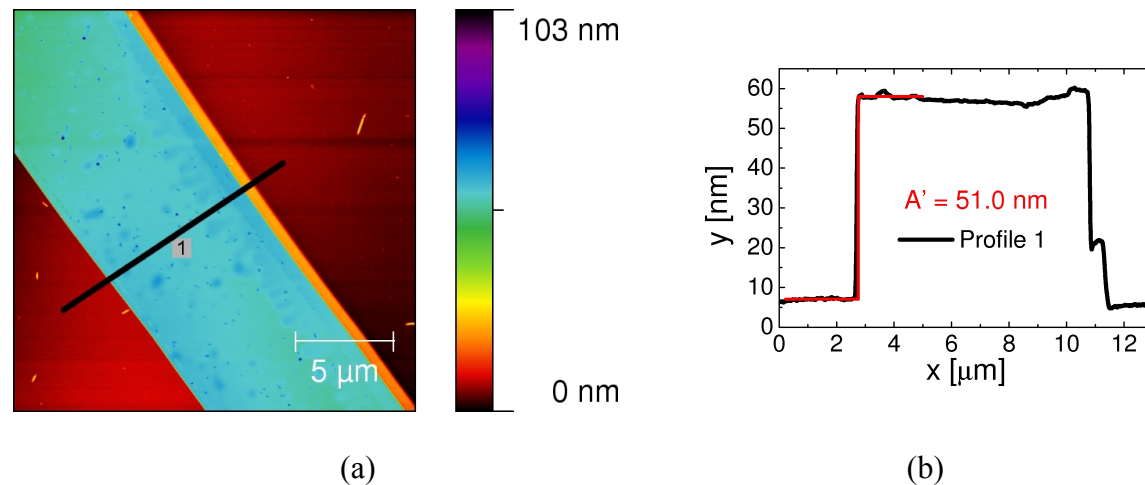


Figure S7. a) Topographic AFM image of the best performing DT-TTF single crystal OFET on a Si/SiO₂. b) The crystal thickness was found to be about 51 nm in Profile 1.

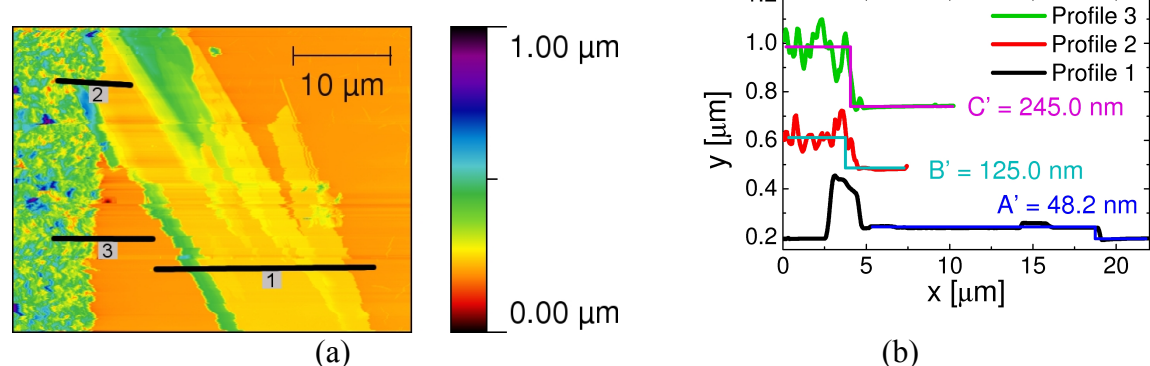


Figure S8. a) Topographic AFM image of a PhCl grown DT-TTF single crystal OFET on a Si/SiO₂ and TTF-TCNQ electrodes. The single crystal melts into the organic electrode.

KPM Analysis:

As reported,^[1] contact resistance $R_{S,D}$ can be determined as $R_{S,D}=W(\Delta V_{S,D})/I_D$ where W is the channel width and ΔV_S and ΔV_D are the potential drops at the source and drain.

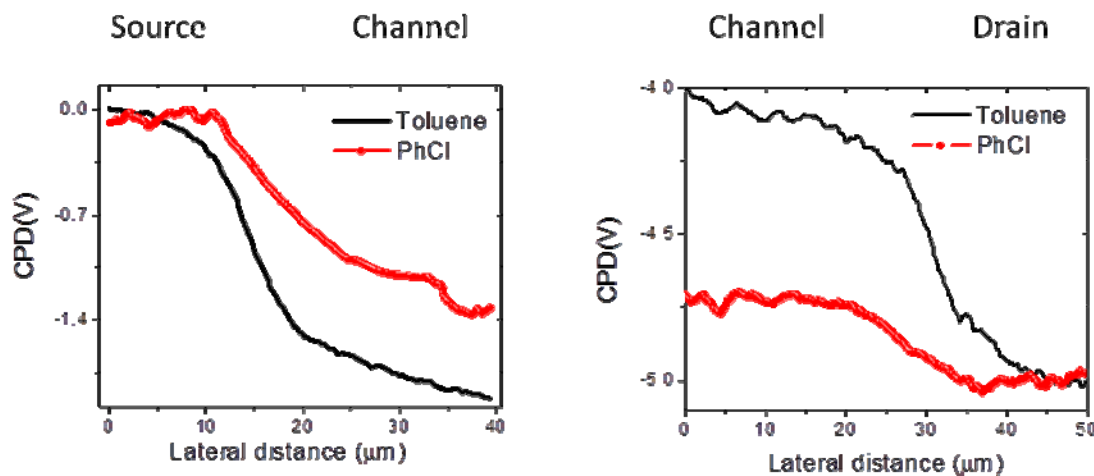


Figure S9. Contact potential difference profile along drain-DT-TTF OSC and source-DT-TTF OSC interface at $V_D=-5\text{V}$ and $V_G=-10\text{V}$.

References:

- [1] L. Bürgi; H. Sirringhaus; R. H. Friend, *Appl. Phys. Lett.* **2002**, *80*, 2913.